Tuned Ternary Quad Subdivision

Tianyun Ni[1] and Ahmad H. Nasri[2]

[1] Dept. CISE, University of Florida
[2] Dept. of Computer Science American University of Beirut

Abstract. A well-documented problem of Catmull and Clark subdivision is that, in the neighborhood of extraordinary point, the curvature is unbounded and fluctuates. In fact, since one of the eigenvalues that determines elliptic shape is too small, the limit surface can have a saddle point when the designer's input mesh suggests a convex shape. Here, we replace, near the extraordinary point, Catmull-Clark subdivision by another set of rules derived by refining each bi-cubic B-spline into nine. This provides many localized degrees of freedom for special rules so that we need not reach out to, possibly irregular, neighbor vertices when trying to improve, or tune the behavior. We illustrate a strategy how to sensibly set such degrees of freedom and exhibit tuned ternary quad subdivision that yields surfaces with bounded curvature, nonnegative weights and full contribution of elliptic and hyperbolic shape components.
Keywords: Subdivision, ternary, bounded curvature, convex hull

1 Introduction

Tuning a subdivision scheme means adjusting the subdivision rules or stencils to obtain a refined mesh and surface with prescribed properties. To date, there exists no subdivision algorithm on quadrilateral meshes that yields bounded curvature while guaranteeing the convex hull property at the extraordinary nodes. This paper proposes ternary refinement to obtain such a scheme. Ternary subdivision offers more parameters in a close vicinity of each extraordinary node to tune the subdivision than binary subdivision does and thereby localizes the tuning. Ternary quad subdivision generalizes the splitting of each quad into nine. If all nodes of a quad are of valence 4, the rules for bi-cubic B-splines shown in Figure 3 are applied and we have C^2 continuity. The challenge is with nodes of valence other than 4, called extraordinary nodes. In particular, we can devise rules at the extraordinary nodes and their newly created direct and diagonal neighbors to achieve

- eigenvalues in order of magnitude as $1, \lambda, \lambda, \lambda^2, \lambda^2, \lambda^2$, $\lambda_i, \dots$ and $0 \le |\lambda_i| < \frac{1}{9}$ for $i = 7, .., 2n+1$; and
- nonnegative weights.

It is possible to get, in addition, $\lambda = 1/3$. Yet, Figure 2 shows that the macroscopic shape of the new scheme and Catmull-Clark are very similar (Figure 2), but, of course, the mesh is denser.

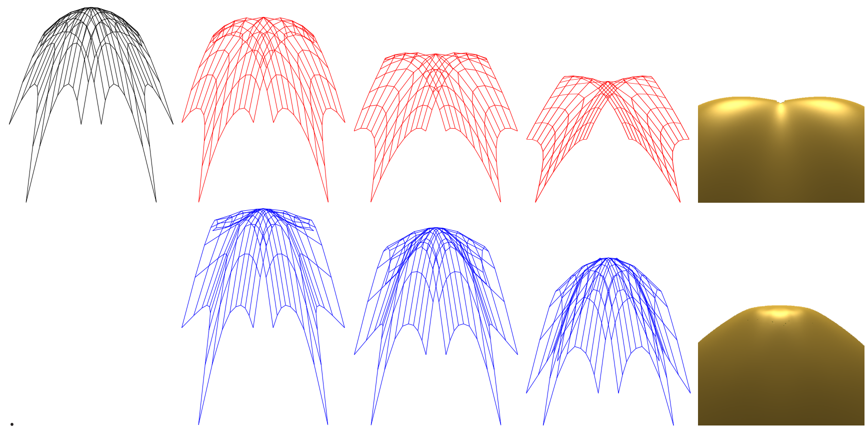

Fig. 1. (*left*) Control net: x, y the characteristic map of Catmull-Clark subdivision and $z = 50(1 - x^2 - 5y^2)$; subdivision steps 3,4,5 and surface for Catmull-Clark subdivision (*top*) and ternary subdivision (*bottom*).

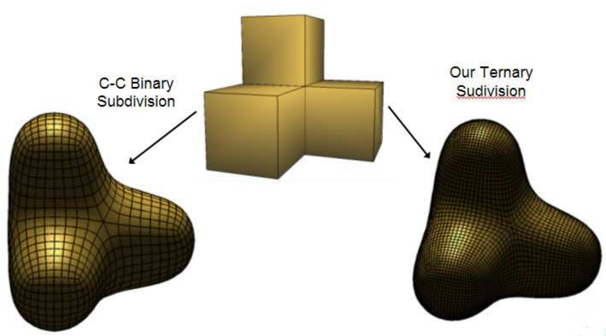

Fig. 2. Three steps of Catmull-Clark subdivision (*left*) and ternary subdivision (*right*).

1.1 Background

Subdivision is a widely adopted tool in computer graphics and is also making inroads into geometric modeling, if only for conceptual modeling. However, [5] pointed out that Catmull-Clark subdivision in particular, is lacking the full set of elliptic and hyperbolic subsubdominant eigenfunctions and therefore *typically* generates saddle shapes in the limit at vertices with valence greater than four (see Figure 1 *top*). This implies that any high-quality (standard, symmetric) scheme needs to have a spectrum $1, \lambda, \lambda, \lambda^2, \lambda^2, \lambda^2$ followed by smaller terms. With the strategy explained in the following, it is possible to achieve such a spectrum by making subdivision stencils near the extraordinary point depend on the valence (Figure 1 *bottom*). While such localized improvement cannot be expected to produce high-quality surfaces in all cases, it is worth seeing whether such improvements can lead to improved rules that are easy to substitute for the known unsatisfactory rules. A major challenge is technical: there are either too few or far too many free parameters occuring in nonlinear inequality constraints. This makes any selection by general optimization [1] impractical. In [3, 4], Loop proposed improvements to his

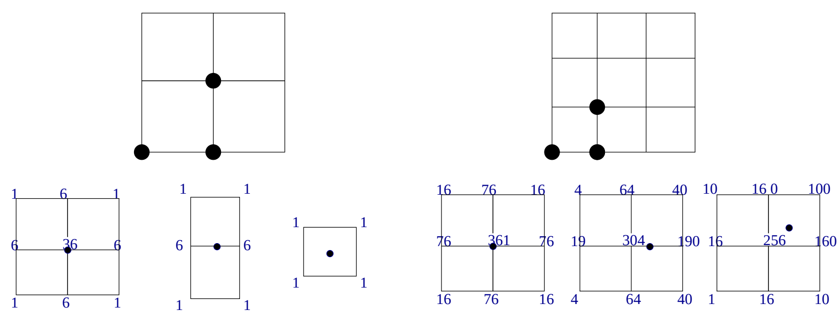

Fig. 3. The regular (bicubic B-spline refinement) stencils of Catmull-Clark (*left*) and ternary quad subdivision (*right*).

well-known triangular scheme on triangular meshes to achieve both bounded curvature for a binary and ternary schemes. To derive weights, he used fixed-degree interpolation of known weights to set *many* unknown weights and reduce the number of free parameters. But quad mesh schemes are far more difficult than triangular mesh schemes since the leading eigenvalues come from a 2 by 2 diagonal block matrix rather than from a 1 by 1 block. They are therefore the roots of quadratic polynomials while, in the case of triangular meshes, the eigenvalue is simple. For n-sided facets, the problem is even more complex due to 4×4 blocks but can be avoided by applying one initial Catmull-Clark subdivision step.

2 Problem Statement

We want to derive a ternary, quad subdivision scheme that is stationary, (rotational and p-mirror) symmetric and affine invariant. Then the leading eigenvalues are, in order of magnitude, $1, \lambda, \lambda, \mu_1, \mu_2, \mu_3$. To achieve bounded curvature, the convex hull property, the eigenvalues and the weights α_i, β_i, γ_i, δ_i and v_i of the ternary quad scheme (see Figure 4) have to satisfy the following constraints:

(i)	C^1 scheme	$1 > \lambda > \mu_i$, and the characteristic map is regular and injective.
(ii)	Bounded Curvature	$\lvert\mu_1\rvert = \lvert\mu_2\rvert = \lvert\mu_3\rvert = \lambda^2$.
(iii)	Convex Hull	$\alpha_i \geq 0, \beta_i \geq 0, \gamma_i \geq 0, \delta_i \geq 0, i = 0..n-1, \quad v_1, v_2 \geq 0,$ $e_0 := 1 - \sum_{i=0}^{n-1}(\alpha_i + \beta_i) \geq 0, f_0 := 1 - \sum_{i=0}^{n-1}(\gamma_i + \delta_i) \geq 0,$ $v_0 := 1 - \sum_{i=1}^{2}(v_i) \geq 0.$
(iv)	Symmetry	$\alpha_l = \alpha_{n-l}, \beta_l = \beta_{n-1-l}, \gamma_l = \gamma_{(n+1-l) \mod n}$, and $\delta_l = \delta_{n-l}$

We focus on the leading eigenvalues and hence the 1-ring of control mesh around extraordinary point and its eigenstructure. As shown in Figure 4, each refinement step generates three types of points corresponding to vertices, edges and faces respectively. Let n be the valence of a generic extraordinary point. We have, offhand, $4n+2$ weights to determine. Symmetry reduces this to $2n+4$ free parameters.

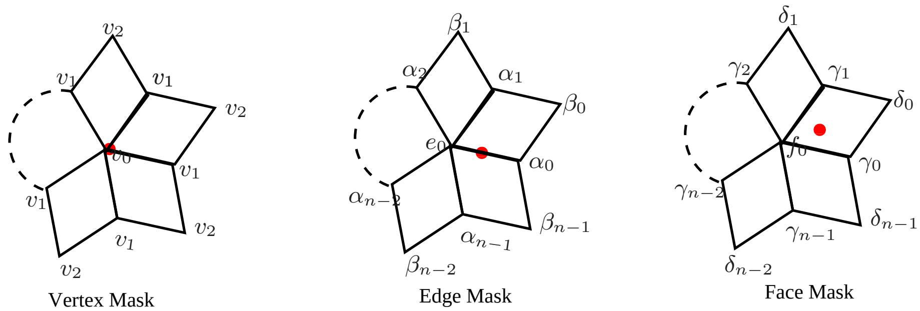

Fig. 4. Refinement stencils used at an extraordinary point .

3 Spectral Analysis

The 1-ring subdivision matrix S with the control vertices shown in Figure 4 is:

$$S := \left(\begin{array}{c|cccccccc} v_0 & v_1 & v_2 & v_1 & v_2 & \cdots & v_1 & v_2 \\ \hline e_0 & \alpha_0 & \beta_0 & \alpha_1 & \beta_1 & \cdots & \alpha_{n-1} & \beta_{n-1} \\ f_0 & \gamma_0 & \delta_0 & \gamma_1 & \delta_1 & \cdots & \gamma_{n-1} & \delta_{n-1} \\ e_0 & \alpha_{n-1} & \beta_{n-1} & \alpha_0 & \beta_0 & \cdots & \alpha_{n-2} & \beta_{n-2} \\ f_0 & \gamma_{n-1} & \delta_{n-1} & \gamma_0 & \delta_0 & \cdots & \gamma_{n-2} & \delta_{n-2} \\ \vdots & \vdots & \vdots & \vdots & \vdots & \ddots & \vdots & \vdots \\ e_0 & \alpha_1 & \beta_1 & \alpha_2 & \beta_2 & \cdots & \alpha_0 & \beta_0 \\ f_0 & \gamma_1 & \delta_1 & \gamma_2 & \delta_2 & \cdots & \gamma_0 & \delta_0 \end{array}\right) \in \mathbb{R}^{(2n+1)\times(2n+1)}.$$

Now denote the discrete Fourier transform of a cyclic sequence $\{\phi_i\}$ by

$$\hat{\phi}_i := \sum_{j=0}^{n-1} \phi_j \omega^{i,j}, \qquad w^{i,j} := e^{\sqrt{-1}\frac{2\pi}{n}ij}.$$

Lemma 1 *The spectrum of S is* $\Lambda = diag(1, \lambda_0^+, \lambda_0^-, \lambda_i^+, \lambda_i^-, \cdots, \lambda_{n-1}^+, \lambda_{n-1}^-)$ *where*

$$\lambda_i^\pm := \frac{(\hat{\alpha}_i + \hat{\delta}_i) \pm \sqrt{(\hat{\alpha}_i - \hat{\delta}_i)^2 + 4\hat{\beta}_i\hat{\gamma}_i}}{2}, \quad i = 1 \ldots n-1. \tag{1}$$

Proof. Since the 2n $\times$ 2n lower block matrix of S is cyclic, we can apply the discrete Fourier transform

$$F := \left(\begin{array}{c|c} 1 & 0 \\ \hline 0 & I_2 \bigotimes (\omega^{i,j}) \end{array}\right)$$

to obtain

$$Q := F^{-1}SF = \left(\begin{array}{c|ccccccc}
v_0 & nv_1 & nv_2 & 0 & 0 & \cdots & 0 & 0 \\ \hline
e_0 & \hat{\alpha}_0 & \hat{\beta}_0 & 0 & 0 & \cdots & 0 & 0 \\
f_0 & \hat{\gamma}_0 & \hat{\delta}_0 & 0 & 0 & \cdots & 0 & 0 \\
e_0 & 0 & 0 & \hat{\alpha}_1 & \hat{\beta}_1 & \cdots & 0 & 0 \\
f_0 & 0 & 0 & \hat{\gamma}_1 & \hat{\delta}_1 & \cdots & 0 & 0 \\
\vdots & \vdots & \vdots & \vdots & \vdots & \ddots & \vdots & \vdots \\
e_0 & 0 & 0 & 0 & 0 & \cdots & \hat{\alpha}_{n-1} & \hat{\beta}_{n-1} \\
f_0 & 0 & 0 & 0 & 0 & \cdots & \hat{\gamma}_{n-1} & \hat{\delta}_{n-1}
\end{array}\right).$$

The eigenvalues $1, \lambda_0^+$, and λ_0^- come from the first 3×3 block. Each 2×2 diagonal block

$$\begin{pmatrix} \hat{\alpha}_i & \hat{\beta}_i \\ \hat{\gamma}_i & \hat{\delta}_i \end{pmatrix}, \qquad i = 1 \ldots n-1,$$

contributes the pair of eigenvalues (1). $\square$

By (iv) and since λ_i^+ and λ_{n-i}^+ are complex conjugate, we anticipate the following lemma.

Lemma 2 $\lambda_i^+ = \lambda_{n-i}^+, \quad \lambda_i^- = \lambda_{n-i}^-, \quad$ *and* $\quad \lambda_i^+, \lambda_i^- \in \mathbb{R}$.

Proof. By symmetry (iv),

$$\hat{\alpha}_i = \alpha_0 + \begin{cases} 2\sum_{j=1}^{\frac{n-1}{2}} \alpha_j \cos\frac{2\pi ij}{n} & \text{if n is odd,} \\ 2\sum_{j=1}^{\frac{n}{2}-1} \alpha_j \cos\frac{2\pi ij}{n} + \alpha_{\frac{n}{2}} \cos \pi i & \text{if n is even.} \end{cases} \tag{2}$$

Since $\cos\frac{2\pi ij}{n} = \cos\frac{2\pi(n-i)j}{n}$ and $\cos(\pi i) = 1$ when i is even, $\hat{\alpha}_i = \hat{\alpha}_{n-i} \in \mathbb{R}$. The same reasoning applies to $\hat{\delta}_i$, $\hat{\beta}_i e^{\frac{\pi}{n}i}$ and $\hat{\gamma}_i e^{-\frac{\pi}{n}i}$ since, e.g.

$$\hat{\beta}_i e^{\frac{\pi}{n}i} = \begin{cases} 2\sum_{j=0}^{\frac{n-1}{2}-1} \beta_j \cos\frac{(2\pi j+\pi)i}{n} + \beta_{\frac{n-1}{2}} \cos \pi i & \text{if n is odd,} \\ 2\sum_{j=0}^{\frac{n}{2}-1} \beta_j \cos\frac{(2\pi j+\pi)i}{n} & \text{if n is even.} \end{cases} \tag{3}$$

Therefore, $\lambda_i^\pm = \lambda_{n-i}^{\pm+} \in \mathbb{R}$ as claimed. $\square$

For $n = 4$ the subdivision stencils are shown in Figure 3. Based on this subdivision matrix, we can compute the matrix Q in Section 3 and therefore compute explicitly the expansions collected in Lemma 3.

Lemma 3 *In the regular setting ($n = 4$),*

$$
\begin{aligned}
[\hat{\alpha}_0^4, \hat{\alpha}_1^4, \hat{\alpha}_2^4, \hat{\alpha}_3^4] &= [\frac{337}{729}, \frac{19}{81}, \frac{1}{9}, \frac{19}{81}],\\
[\hat{\beta}_0^4 e^{\frac{\pi}{n}i}, \hat{\beta}_1^4 e^{\frac{\pi}{n}i}, \hat{\beta}_2^4 e^{\frac{\pi}{n}i}, \hat{\beta}_3^4 e^{\frac{\pi}{n}i}] &= [\frac{88}{729}, \frac{4\sqrt{2}}{81}, 0, -\frac{4\sqrt{2}}{81}],\\
[\hat{\gamma}_0^4 e^{-\frac{\pi}{n}i}, \hat{\gamma}_1^4 e^{-\frac{\pi}{n}i}, \hat{\gamma}_2^4 e^{-\frac{\pi}{n}i}, \hat{\gamma}_3^4 e^{-\frac{\pi}{n}i}] &= [\frac{352}{729}, \frac{16\sqrt{2}}{81}, 0, -\frac{16\sqrt{2}}{81}],\\
[\hat{\delta}_0^4, \hat{\delta}_1^4, \hat{\delta}_2^4, \hat{\delta}_3^4] &= [\frac{121}{729}, \frac{11}{81}, \frac{1}{9}, \frac{11}{81}]. \qquad (4)
\end{aligned}
$$

4 Deriving Weights by Interpolating the Regular Case

The idea of deriving extraordinary rules is inspired by Loop's approach [4]. First, we interpolate the regular stencil by a polynomial. Such a polynomial, say β^n, will be evaluated to define the coefficients β_i^n. For $n = 4$, due to symmetry, the constraints on the polynomial β^n are $\beta^n(\cos\frac{\pi}{n}) = \frac{40}{729}$ and $\beta^n(\cos\frac{3\pi}{n}) = \frac{4}{729}$. The linear interpolant to these values is negative on some subinterval of $[-1, 1]$ and therefore cannot give suitable coefficients $\beta_i^n \geq 0$ for $n > 4$. Adding the constraint $\beta^n(-1) = 0$ yields the polynomial

$$
\beta^4(t) := \frac{1}{729}\left((44 - 18\sqrt{2})(1-t)^2 + (44 - 9\sqrt{2})2t(1-t) + (36\sqrt{2})t^2\right)
$$

which is nonnegative on $[-1, 1]$. We conjecture the general formulae for arbitrary n based on the polynomials of the same low degree and choose

$$
\begin{aligned}
&\alpha^n(t) := a_{n,1}\Big((t + b_{n,1})^2 + c_{n,1}\Big), \quad \beta^n := \frac{4}{n}\beta^4, \quad \gamma^n := \frac{16}{n}\beta^4,\\
&\delta^n(t) := a_{n,4}\Big((t + b_{n,4})^2 + c_{n,4}\Big). \qquad (5)
\end{aligned}
$$

Now, we predict the general formulae for any $n > 4$ by evaluating the polynomials at the x-component of points equally distributed over the unit circle. This yields two of the three types of stencils at the extraordinary point and leaves, as degrees of freedom, the coefficients depending on n in (5).

Lemma 4 *The subdivision rules, for valence n and $j = 0 \ldots n-1$ can be chosen as*

$$
\alpha_j^n := \alpha^n(u), \quad \delta_j^n := \delta^n(u), \quad u := \cos\frac{2\pi j}{n}, \qquad (6)
$$

$$
\beta_j^n := \beta^n(v_+), \quad v_+ := \cos\frac{2\pi j + \pi}{n}, \qquad \gamma_j^n := \gamma^n(v_-), \quad v_- = \cos\frac{2\pi j - \pi}{n}
$$

where

$$a_{n,1} := \frac{4}{n}\hat{\alpha}_2^n, \quad b_{n,1} := \frac{\hat{\alpha}_1^n}{n a_{n,1}}, \quad a_{n,4} := \frac{4}{n}\hat{\delta}_2^n, \quad b_{n,4} := \frac{\hat{\delta}_1^n}{n a_{n,4}}. \tag{7}$$

Note that, together with β and γ, equations (7) yield explicit expressions for $\lambda_1^{\pm}$ and $\lambda_2^{\pm}$ in terms of the the coefficients $a_{n,1}$, $b_{n,1}$, $c_{n,1}$, $a_{n,4}$, $b_{n,4}$, $c_{n,4}$.

Proof. By symmetry, the weights are a discrete cosine transformation of their Fourier coefficients:

$$\alpha_i^n = \frac{1}{n}\sum_{j=0}^{n-1}\hat{\alpha}_j^n \cos\frac{2\pi ij}{n}, \qquad \beta_i^n = \frac{1}{n}\sum_{j=0}^{n-1}\hat{\beta}_j'^n \cos\frac{2\pi ij + \pi j}{n}, \tag{8}$$
$$\gamma_i^n = \frac{1}{n}\sum_{j=0}^{n-1}\hat{\gamma}_j'^n \cos\frac{2\pi ij - \pi j}{n}, \qquad \delta_i^n = \frac{1}{n}\sum_{j=0}^{n-1}\hat{\delta}_j^n \cos\frac{2\pi ij}{n}.$$

For $n = 4$, we verify the consistency of the choice (6) by substituting (4) into (8).

$$\alpha_i^4 = \frac{1}{18}\big((u + \frac{19}{18})^2 + \frac{151}{324}\big), \qquad \delta_i^4 = \frac{1}{18}\big((u + \frac{11}{18})^2 - \frac{41}{324}\big).$$

Next, we decompose the polynomial into a vector of basis functions and a vector of coefficients:

$$a_{n,1}\Big((u+b_{n,1})^2+c_{n,1}\Big) = [1, u, 2u^2-1][a_{n,1}b_{n,1}^2+\frac{1}{2}a_{n,1}+a_{n,1}c_{n,1}, 2a_{n,1}b_{n,1}, \frac{1}{2}a_{n,1}]^T.$$

We mimic this decompostion for $n > 4$, by choosing $\hat{\alpha}_i^n = 0$ for $2 < i < n-2$. Then

$$\alpha_i^n = \frac{1}{n}\sum_{j=0}^{n-1}\hat{\alpha}_j^n \cos\frac{2\pi ij}{n} = [1, \cos\frac{2\pi i}{n}, \cos\frac{4\pi i}{n}][\frac{1}{n}\hat{\alpha}_0^n, \frac{2}{n}\hat{\alpha}_1^n, \frac{2}{n}\hat{\alpha}_2^n]^T.$$

Since $\cos\frac{2\pi i}{n} = u$, we have $\cos\frac{4\pi i}{n} = 2u^2 - 1$ and comparison of terms yields

$$2a_{n,1}b_{n,1} = \frac{2}{n}\hat{\alpha}_1^n, \quad \text{and} \quad \frac{1}{2}a_{n,1} = \frac{2}{n}\hat{\alpha}_2^n.$$

Solving $a_{n,1}, b_{n,1}$ in terms of $\hat{\alpha}_1^n, \hat{\alpha}_2^n, n$, and similarly for δ_i^n, yields (7). □

The rules of Lemma 4 preserve rotational and p-mirror symmetry. For $n > 4$, they reduce the free parameters from $2n + 4$ to six, namely $a_{n,i}, b_{n,i}, c_{n,i}, i = 1, 4$. (For $n = 3$ we use the original $2n + 4 = 10$ free parameters to enforce $\lambda_1^+ = \lambda, \quad \lambda_1^- = \lambda^2, \quad \lambda_0^+ = \lambda^2, \quad \lambda_0^- < \lambda^2$.) It remains need to determine the six free parameters so that for $n > 4$ the weigths $\alpha_j, \delta_j, v_1, v_2, e_0, f_0, v_0$ are nonnegative (β_j and γ_j are nonnegative since $\beta^4 \geq 0$ on $[-1, 1]$) and

$$\begin{aligned} \Lambda &= \mathrm{diag}(1, \lambda_1^+, \lambda_{n-1}^+, \lambda_2^+, \lambda_{n-2}^+, \lambda_0^+, \nu_1, \nu_2, \dots, \nu_{2n-5}) \\ &= \mathrm{diag}(1, \lambda, \lambda, \lambda^2, \lambda^2, \lambda^2, \dots, \lambda_i, \dots), \quad \text{where} \quad 0 < |\lambda_i| < \lambda^2. \end{aligned} \tag{9}$$

By (1), and since $\hat{\gamma}_k$ and $\hat{\beta}_k$ are fixed, each of the constraints $\lambda_1^+ = \lambda$ and $\lambda_2^+ = \lambda^2$ is an equation in the parameters, $a_{n,1}$, $b_{n,1}$, $a_{n,4}$, $b_{n,4}$, explicitly so due to (7). The additional necessary constraint, $\lambda_0^+ = \lambda^2, \lambda_0^- < \lambda^2$ is enforced by choice of v_1, v_2 in the first 3 by 3 block of Q. The result is an underconstrained system with linear inequality constraints. We find, for example, the closed-form solution for $n = 5 \ldots 10$ stated in Lemma 5 and yielding the elliptic and saddle shapes shown in Figure 7.

Lemma 5 *For $n = 5..10$, the following choice satisfies (i)-(iv) and $\lambda = 1/3$:*

$$\begin{aligned} a_{n,1} &= \frac{.413}{n}, \quad b_{n,1} = .624, \quad c_{n,1} = .229 \\ a_{n,4} &= \frac{.260}{n}, \quad b_{n,4} = .286, \quad c_{n,4} = .058 \end{aligned} \tag{10}$$

Proof. We need only verify (i), (ii) and (iii) listed in Section 2 since the scheme is symmetric by construction. Table 1 shows all eigenvalues other than $1, \frac{1}{3}, \frac{1}{3}, \frac{1}{9}, \frac{1}{9}, \frac{1}{9}$ for $n = 3 \ldots 10$. In particular, $\lambda_1 = \lambda_{n-1} = \frac{1}{3}$ is the subdominant eigenvalue. Table 2 verifies nonnegative weights summing to 1. The u-differences, scaled to unit size, fall strictly into the lower right quadrant and, by symmetry, the v-differences fall strictly into the upper right quadrant (Figure 6). The partial derivatives are a convex combination of the differences and hence all pairwise crossproducts are strictly positive. By [8], the characteristic map is regular. In addition, as shown in Figure 5, the first half-segment of the control net does not intersect the negative x-axis. By the convex hull property and [7] Theorem 21, injectivity of the characteristic map follows. $\square$

ν_i	n=3	n=4	n=5	n=6	n=7	n=8	n=9	n=10
ν_1	-.063	.037	.057	.057	.057	.057	.057	.057
ν_2	$\cdots$	.037	.057	.057	.057	.057	.057	.057
ν_3	$\cdots$	.012	-.023	-.012	-.002	.009	.019	.030
ν_4	$\cdots$	$\cdots$	-.001	-.001	-.001	-.001	-.001	-.001
ν_5	$\cdots$	$\cdots$	-.001	-.001	-.001	-.001	-.001	-.001
ν_6	$\cdots$	$\cdots$	$\cdots$	ϵ	ϵ	ϵ	ϵ	ϵ
ν_7	$\cdots$	$\cdots$	$\cdots$	ϵ	ϵ	ϵ	ϵ	ϵ
ν_8	$\cdots$	$\cdots$	$\cdots$	$\cdots$	ϵ	ϵ	ϵ	ϵ
ν_9	$\cdots$	$\cdots$	$\cdots$	$\cdots$	ϵ	ϵ	ϵ	ϵ
ν_{10}	$\cdots$	$\cdots$	$\cdots$	$\cdots$	$\cdots$	ϵ	ϵ	ϵ
ν_{11}	$\cdots$	$\cdots$	$\cdots$	$\cdots$	$\cdots$	ϵ	ϵ	ϵ
ν_{12}	$\cdots$	$\cdots$	$\cdots$	$\cdots$	$\cdots$	$\cdots$	ϵ	ϵ
ν_{13}	$\cdots$	$\cdots$	$\cdots$	$\cdots$	$\cdots$	$\cdots$	ϵ	ϵ
ν_{14}	$\cdots$	$\cdots$	$\cdots$	$\cdots$	$\cdots$	$\cdots$	$\cdots$	ϵ
ν_{15}	$\cdots$	$\cdots$	$\cdots$	$\cdots$	$\cdots$	$\cdots$	$\cdots$	ϵ

Table 1. Eigenvalues (see 9) other than $1, \frac{1}{3}, \frac{1}{3}, \frac{1}{9}, \frac{1}{9}, \frac{1}{9}$ for $n = 3..10$. $\quad 0 < |\epsilon| < .001$

The main contribution of the paper is technical: to provide a manageable set of parameters that make it easy to satisfy the formal constraints (i)–(iv). This set can be further pruned by minimizing regions of meshes where the scheme exhibits hybrid behavior [5], i.e. the Gauss curvature is not uniquely of one sign in the limit. It should be noted that this is typically not enough to guarantee surface fairness, for example to avoid undue flatness when convexity is indicated by the control mesh.

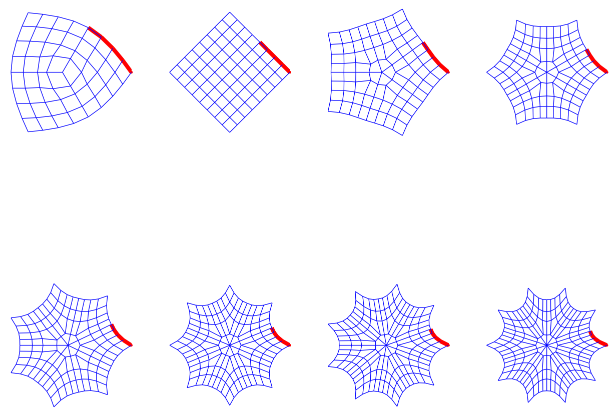

Fig. 5. Control polyhedron of the characteristic map for $n = 3..10$. Injectivity test: each red fat segment does not intersect the negative x-axis.

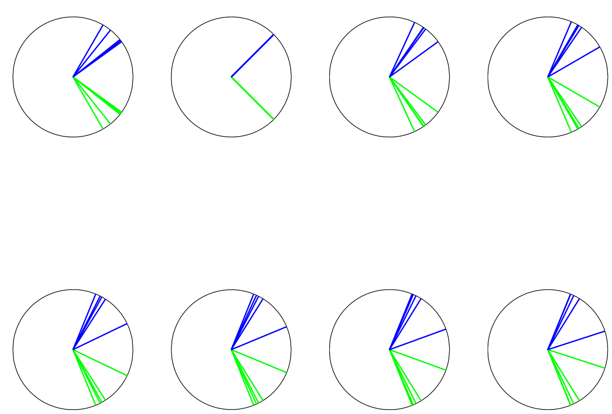

Fig. 6. The normalized differences in the u direction (*green*) and v direction (*blue*).

weights	n=3	n=4	n=5	n=6	n=7	n=8	n=9	n=10
v_0	.524	.495	.460	.470	.481	.491	.502	.512
v_1	.119	.104	.098	.078	.064	.053	.044	.038
v_2	.040	.022	.010	.010	.010	.010	.010	.010
e_0	.550	.417	.417	.417	.417	.417	.417	.417
α_0	.291	.261	.237	.198	.169	.148	.132	.119
β_0	.062	.055	.047	.042	.037	.033	.030	.027
α_1	.009	.088	.091	.103	.105	.103	.099	.094
β_1	.018	.005	.012	.017	.019	.020	.020	.020
α_2	$\cdots$	.026	.022	.017	.023	.032	.040	.045
β_2	$\cdots$	$\cdots$	.000	.002	.004	.007	.009	.010
α_3	$\cdots$	$\cdots$	$\cdots$	.025	.018	.012	.011	.014
β_3	$\cdots$	$\cdots$	$\cdots$	$\cdots$	.000	.001	.002	.003
α_4	$\cdots$	$\cdots$	$\cdots$	$\cdots$	$\cdots$	.019	.015	.011
β_4	$\cdots$	$\cdots$	$\cdots$	$\cdots$	$\cdots$	$\cdots$	.000	.000
α_5	$\cdots$	$\cdots$	$\cdots$	$\cdots$	$\cdots$	$\cdots$	$\cdots$	.015
f_0	.309	.351	.351	.351	.351	.351	.351	.351
δ_0	.180	.137	.089	.074	.063	.056	.049	.044
$\gamma_1 = \gamma_0$	.226	.219	.191	.167	.148	.132	.118	.108
δ_1	.017	.014	.021	.029	.033	.034	.034	.033
γ_2	.023	.022	.050	.068	.077	.080	.080	.079
δ_2	$\cdots$	.001	.017	.004	.002	.005	.008	.011
γ_3	$\cdots$	$\cdots$	.000	.006	.017	.027	.035	.041
δ_3	$\cdots$	$\cdots$	$\cdots$	.024	.000	.008	.003	.002
γ_4	$\cdots$	$\cdots$	$\cdots$	$\cdots$	.078	.003	.007	.013
δ_4	$\cdots$	$\cdots$	$\cdots$	$\cdots$	$\cdots$	.018	.014	.009
γ_5	$\cdots$	$\cdots$	$\cdots$	$\cdots$	$\cdots$	$\cdots$	.000	.001
δ_5	$\cdots$	$\cdots$	$\cdots$	$\cdots$	$\cdots$	$\cdots$	$\cdots$	.015

Table 2. The subdivision rule according to Lemma 5 has non-negative weights. $0 < \epsilon < .001$

Acknowledgment: This work was supported by NSF Grant CCF-0430891 and American University of Beirut URB-2006. Jörg Peters gave valuable technical guidance and assistance.

References

1. L. Barthe, and L. Kobbelt, Subdivision Scheme tuning around extraordinary vertices, *Computer Aided Geometric Design, 21: 561-583.*
2. E. Catmull, and J. Clark, Recursively Generated B-spline Surfaces on Arbitrary Topological Meshes. *Computer Aided Design, 10(6): 350-355.*(1978)
3. C. Loop, Smooth Ternary Subdivision of Triangle Meshes *Curve and Surface Fitting* (Saint-Malo, 2002).
4. C. Loop, Bounded curvature triangle Mesh subdivision with the convex hull property. *The Visual Computer, 18 (5-6), 316-325.*
5. K. Karciauskas, J. Peters and U. Reif, Shape Characterization of Subdivision Surfaces – Case Studies, *Comp. Aided Geom. Design*, 21(6), 2004, 601–614.

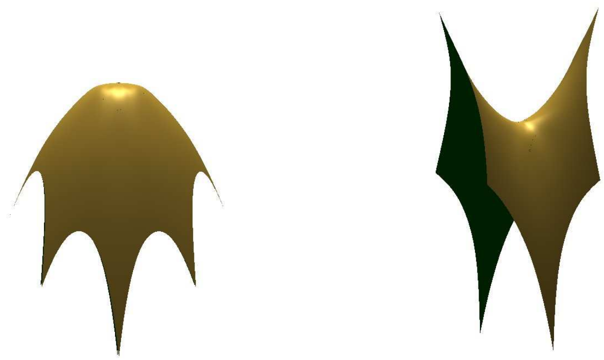

Fig. 7. Surfaces generated by the rules of Lemma 5.

6. A. Nasri, I. Hasbini, J. Zheng, T. Sederberg, Quad-based Ternary Subdivision, presentation Dagstuhl Seminar on Geometric Modeling, 29 May - 03 June, 2005
7. U. Reif and J. Peters. Structural Analysis of Subdivision Surfaces – A Summary *Topics in Multivariate Approximation and Interpolation*, Elsevier Science Ltd, K. Jetter et al., 2005, 149–190.
8. G. Umlauf, Analysis and Tuning of Subdivision Algorithms. *Proceedings of the 21st spring conference on Computer Graphics, 33-40.* (2005)